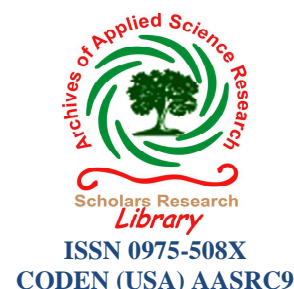




Scholars research library

Archives of Applied Science Research, 2011, 3 (5):491-497

(<http://scholarsresearchlibrary.com/archive.html>)



Magnetic properties of $\text{Li}_x\text{Mg}_{0.7-2x}\text{Zn}_{0.3}\text{Fe}_{2+x}\text{O}_4$ synthesized using sucrose precursor

M.K.Rendale^a, S. D. Kulkarni^b and Vijaya Puri*^c

^aDepartment of Engineering Physics, Hirasugar Institute of Technology, Nidasoshi, India

^bCenter for Materials Characterization, National Chemical Laboratory, Pune, India

^cThick and Thin film Device Lab, Department of Physics, Shivaji University, Kolhapur, India

ABSTRACT

$\text{Li}_x\text{Mg}_{0.7-2x}\text{Zn}_{0.3}\text{Fe}_{2+x}\text{O}_4$ ferrites were synthesized by the sucrose precursor method. The co-substitution of lithium and iron ions caused a contraction in the lattice parameter obeying Vegard's law. The variation in force constant with bond length showed an unexpected trend on both A and B sites of the lattice. Magnetic hysteresis studies revealed a decrease in the squareness of the loop with reduction in magnetization due to the increase in Mg^{2+} concentration. AC Susceptibility studies revealed the possibility of presence of single domain and superparamagnetic particles in the samples. The Curie temperature T_c decreased with the increase in magnesium concentration.

Key words : $\text{Li}_x\text{Mg}_{0.7-2x}\text{Zn}_{0.3}\text{Fe}_{2+x}\text{O}_4$; Sucrose precursor; Hysteresis; A. C. Susceptibility.

INTRODUCTION

Lithium ferrite devices find extensive applications in microwave technology as microwave absorbers, isolators, circulators, phase shifters, latching devices etc, because of their non-reciprocal microwave property, high saturation magnetization, squareness of hysteresis loop, high resistivity [1,2,3]. In addition to these properties, their cost effectiveness and superior high temperature performances due to high T_c , make the Li-ferrites to score over garnets in respect of their use in advanced technology.

It is well established that the structural, magnetic and electric properties of these ferrites may suitably be modified to serve different purposes by introducing different substituents and by controlled preparative conditions [4]. The substitution of zinc with 0.3 formula unit in spinel ferrites would lead high resistivity in the material, besides improving the magnetic properties

[5,6]. Magnesium ferrites also play their role in the developing microwave technology as a class of microwave ferrites [7]. However no such studies have been reported so far on magnesium substituted lithium-zinc ferrites with zinc content unaltered. In view of this, our investigation is focused on characterization, hysteresis and A.C. susceptibility studies of a series of Li-Mg-Zn ferrites with the composition formula, $\text{Li}_x\text{Mg}_{0.7-2x}\text{Zn}_{0.3}\text{Fe}_{2+x}\text{O}_4$ synthesized using sucrose precursor [8], which gives rise to nano size particles.

MATERIALS AND METHODS

The Li-Mg-Zn nano ferrites with the compositional formula $\text{Li}_x\text{Mg}_{0.7-2x}\text{Zn}_{0.3}\text{Fe}_{2+x}\text{O}_4$ where, $X=0, 0.07, 0.14, 0.21, 0.28$ and 0.35 were synthesized by chemical route using metal nitrates and sucrose precursor. The ferrite powders were mixed with Bi_2O_3 of about 0.5 % by weight to avoid excess evaporation of lithium and zinc during sintering process. Each of the mixtures was ground well using mortar and pestle for an hour and then sintered at 800°C for 8 hours followed by subsequent slow cooling to room temperature.

The X-ray diffraction for all the powder samples was studied using Cu-K_α radiation ($\lambda=1.5425 \text{ \AA}$) on a PHILIPS PW-3710 diffractometer with the angle 2θ between 20° and 80° . The IR-absorption spectra at room temperature was recorded in the wave number range of 300 to 700 cm^{-1} using a Fourier transform infrared (FTIR) spectrophotometer (Perkin Elmer-Spectrum 2000). Magnetic B-H measurements were carried out at room temperature using the vibration sample magnetometer [EG and G, PAR-4500] with the field strength up to $10,000 \text{ Oe}$. The measurement of ac susceptibility as a function of temperature was carried out using a double coil apparatus operating at 263 Hz in a rms field of 7 Oe .

RESULTS AND DISCUSSION

1. Structural studies

Typical X-ray diffractogram of the ferrite sample with composition $X=0.21$ is shown in figure 1.

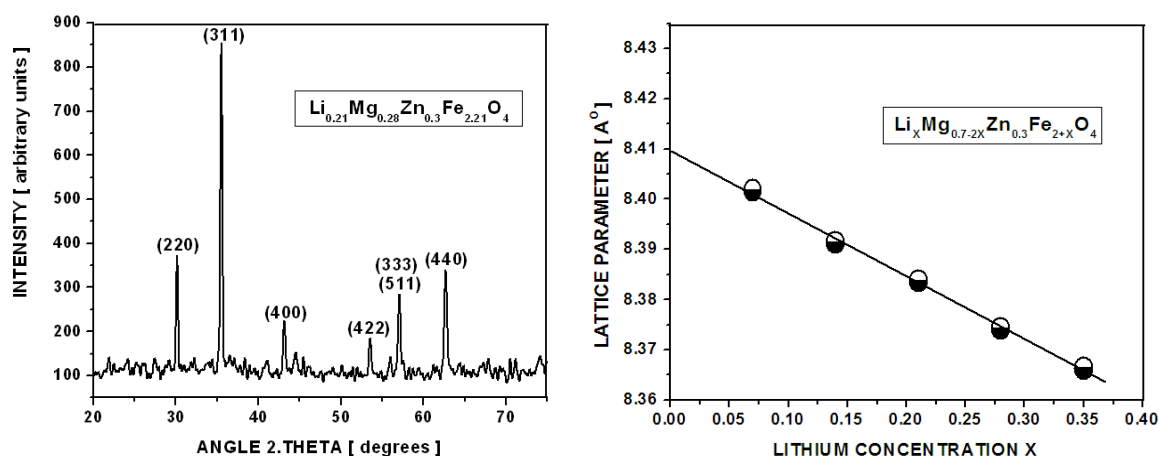


Fig. 1. X-ray diffractogram of $\text{Li}_{0.21}\text{Mg}_{0.28}\text{Zn}_{0.3}\text{Fe}_{2.21}\text{O}_4$ and variation of lattice parameter of the $\text{Li}_x\text{Mg}_{0.7-2x}\text{Zn}_{0.3}\text{Fe}_{2+x}\text{O}_4$ with lithium concentration X.

The X-ray diffraction shows well-defined reflections revealing the formation of single phase cubic spinel ferrites. The lattice parameter has been determined by using Bragg's equation for first order diffraction as $a = \lambda \sqrt{(h^2+k^2+l^2)} / 2\sin\theta$ where, λ is wavelength of the incident X-ray radiation and θ , a half of the diffraction angle 2θ .

The lattice parameter shows a linear reduction in its value with the increase in lithium content due to difference in ionic sizes. The smaller ionic radii Li^{1+} (0.71 \AA) and Fe^{3+} (0.67 \AA) ions replace Mg^{2+} (0.78 \AA) ions causing a contraction in the cube edge of the unit cell. The cation radii r_A and r_B were estimated from the powder X-ray diffraction pattern using the formulae, $r_A = [U - 0.25] a \sqrt{3} - r_o$ and $r_B = [0.625 - U] a - r_o$.

Where, $r_o = 1.35 \text{ \AA}$, the radius of oxygen ion(anion) and $U = 0.3819$, the anion parameter taken as the average of U-parameter values for Mg-Zn and Li-Zn ferrites.

The data of X-ray density and cation radius on A and B-sites are tabulated in table 1.

Table 1. X-ray density, Cation radii on A and B-sites and IR absorption band edges for the $\text{Li}_x\text{Mg}_{0.7-2x}\text{Zn}_{0.3}\text{Fe}_{2+x}\text{O}_4$ ferrite.

Li content X	ρ g/cc	$r_A \text{ \AA}$	$r_B \text{ \AA}$	$\nu_1 \text{ cm}^{-1}$	$\nu_2 \text{ cm}^{-1}$
0.00	4.7138	0.5753	0.6987	553.28	411.23
0.07	4.7796	0.5694	0.6925	565.85	409.99
0.14	4.8197	0.5670	0.6899	569.95	401.54
0.21	4.8552	0.5653	0.6881	577.91	396.81
0.28	4.8942	0.5631	0.6857	589.81	389.41
0.35	4.9306	0.5613	0.6838	589.57	387.26

The observed contraction in cation radii r_A and r_B with Li-content provides an evidence for the differences in ionic radii [4].

The observation on X-ray density of the ferrite samples reveals an increasing trend with Li-content. This is because of the increase in atomic weight and considerable reduction in volume due to ionic size differences. The average size of the particles calculated using width of (311)-peak lies within the range of 52 to 84 nm. It is observed that the average size of the particles remains almost independent of the lithium content.

The I.R. spectrogram for the ferrite sample with $X=0.21$ is shown in figure2.

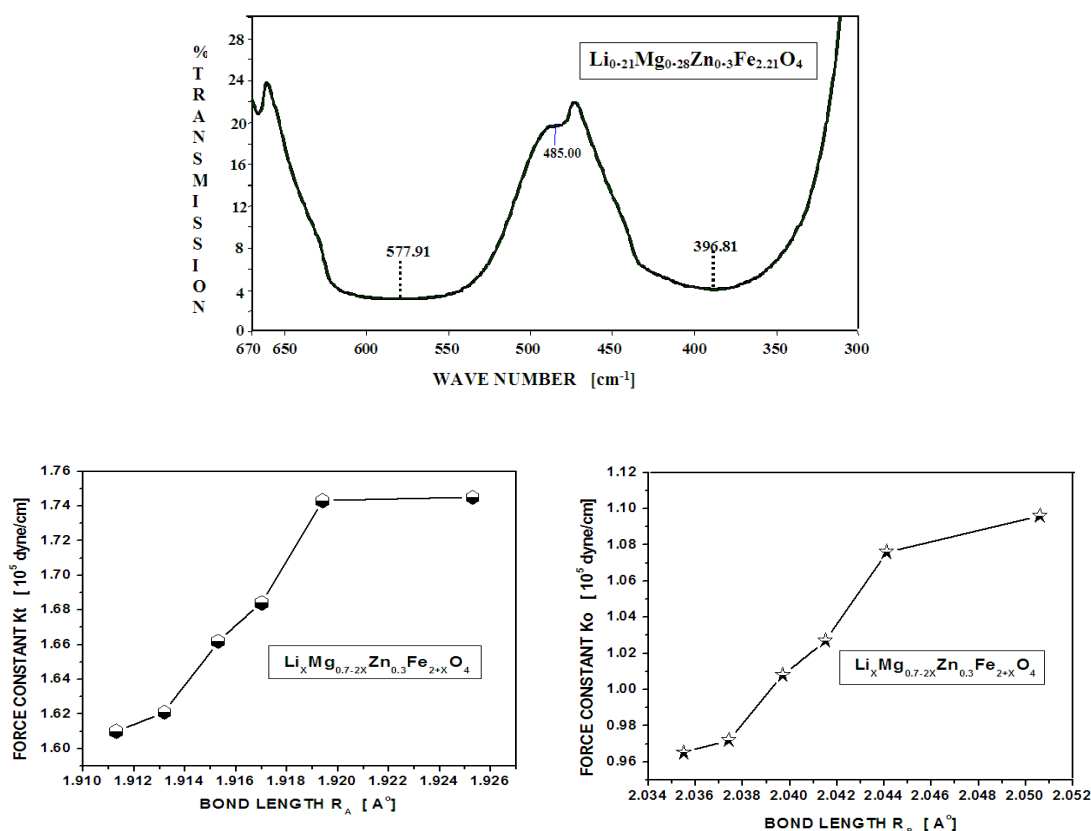


Fig. 2. IR spectrogram of $\text{Li}_x\text{Mg}_{0.7-2x}\text{Zn}_{0.3}\text{Fe}_{2+x}\text{O}_4$ along with variation of tetrahedral force constant Kt and octahedral force constant Ko

All the samples exhibited two prominent absorption bands at the wave numbers ν_1 and ν_2 between 600cm^{-1} and 380cm^{-1} respectively as expected for spinel ferrites. The experimental error in the measurement of the band peaks is $\sim \pm 0.02\%$. The observed shift in the value of ν_1 and ν_2 slightly towards higher and lower frequencies respectively with the increase in lithium content as evident from table 1, may be due to the vibrations of ' $\text{Fe}^{3+}\text{-O}^{2-}$ ' complexes on A and B-sites respectively. The variations of force constants with the bond lengths are also shown in the figure 2. The force constants for tetrahedral and octahedral sites Kt and Ko respectively were calculated from the IR spectra using the standard procedure and formulae suggested in the literature [9,10]. The extension in bond length normally leads to the reduction in force constant [11]. However, the present case reports an unexpected result that force constants increase with extension in bond lengths. Similar anomalous relationship between force constant and metal-oxygen bond length was also reported in the literature [11-13]. They have attributed their anomalous results to the fact that "under favourable conditions, oxygen ion can form stronger bonds with metal ions even at larger internuclear separations".

2. Magnetic properties

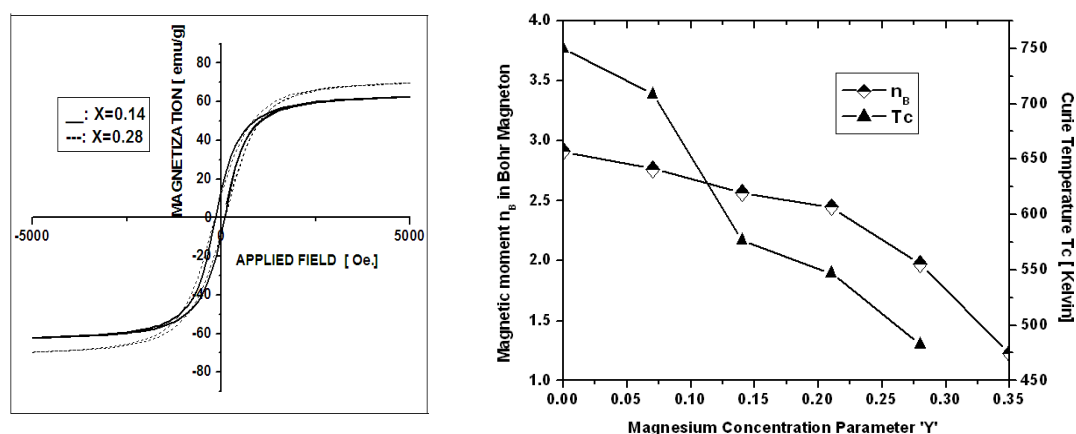


Fig. 3. Magnetic hysteresis loops and variation of magnetic moment n_B and Curie temperature T_c with magnesium composition parameter Y

The magnetic measurements in the present work were taken at room temperature. The hysteresis curves for the samples with $X=0.14$ and $X=0.28$ are presented in the figure 3.

The present case reports that, the increase in magnesium concentration decreases the squareness of the hysteresis loop, which may be the indication of fall in the value of negative anisotropy of the material. The slight increase in the value of remanence ratio M_R/M_S with the Mg^{2+} concentration is also observed, which supports the statement of reduction in anisotropy of the material. The observed decrease in the value of coercivity with the increase in Mg^{2+} concentration may be due to the reduction in the value of anisotropy constant K_1 . Generally, the ferrites which possess square hysteresis loop are found to have more negative value for anisotropy constant K_1 [14].

For the series of ferrite samples under study the cation distribution formula may be written as , $[Zn^{2+}_{0.3} Mg^{2+}_{\delta} Fe^{3+}_{0.7-\delta}]_A [Li^{1+}_{0.35-Y} Mg^{2+}_{2Y-\delta} Fe^{3+}_{1.65-Y+\delta}]_B O_4$ where $Y = 0.35 - X$ is the concentration parameter of Mg^{2+} ions. According to this formula, as the parameter Y increases the concentration of non-magnetic Mg^{2+} ions increases, due to which the number of $Fe_A^{3+}-O^{2-}-Fe_B^{3+}$ magnetic bonds decreases resulting in a reduction in the normalized magnetization of both the A and B-sublattices. But the Mg^{2+} ions predominantly enter B-sites, hence the substitution of Mg^{2+} ions replace Li^{1+} and Fe^{3+} ions from B-sites, thereby reducing the normalized magnetization of B-sites considerably. This results in the net magnetization M_S or magnetic moment per molecule in Bohr magneton n_B of the material to decrease with Mg^{2+} concentration parameter Y as shown in figure 3. The data of magnetic properties are given in table 2. The experimental errors in M_S and H_c measurements are $\pm 1.1\%$ and $\pm 0.1\%$ respectively. The remanence ratio M_R / M_S and coercivity H_c depend on the three basic material properties, viz, microstructure, magneto-crystalline anisotropy and stress sensitivity. Each of these can have profound effect on the loop shape either independently or combined. The remanence ratio diminishes, while, coercivity gets magnified with enhanced anisotropy of the material [15].

Table 2. Saturation magnetization M_s , Remanence ratio M_R/M_S , Coercivity H_c of $i_X\text{Mg}_{0.7-2X}\text{Zn}_{0.3}\text{Fe}_{2+X}\text{O}_4$

Li content X	M_s emu/g	M_R/M_S	H_c Oe.
0.00	32.26	0.256	142.37
0.07	51.68	0.230	145.1
0.14	63.8	0.220	147.36
0.21	66.53	0.184	148.2
0.28	71.36	0.171	152.36
0.35	74.85	0.165	161.8

The typical curves indicating the variation of normalized A.C. Susceptibility with temperature for the ferrite samples with $X=0.07, 0.14, 0.21$ and 0.28 are given in figure 4. From the AC susceptibility studies, it is observed that, for the ferrite with $X=0$ and 0.07 , the normalized susceptibility sharply decreases with increasing temperature and drops to zero at the Curie temperature T_c , which indicates that the samples may possess the superparamagnetic particles [16]. While for the other samples with $X=0.14, 0.21, 0.28$ and 0.35 a peak near T_c is obtained indicating the possibility of presence of single domain particles in the material [17]. The Curie temperature values obtained by AC susceptibility studies are plotted against the magnesium concentration parameter 'Y' in the figure 3 along with magnetic moment. The observed lowering in T_c with Y is attributed to the weakening of A-B interaction occurring due to the replacement of Fe^{3+} ions by Mg^{2+} ions on B-sites.

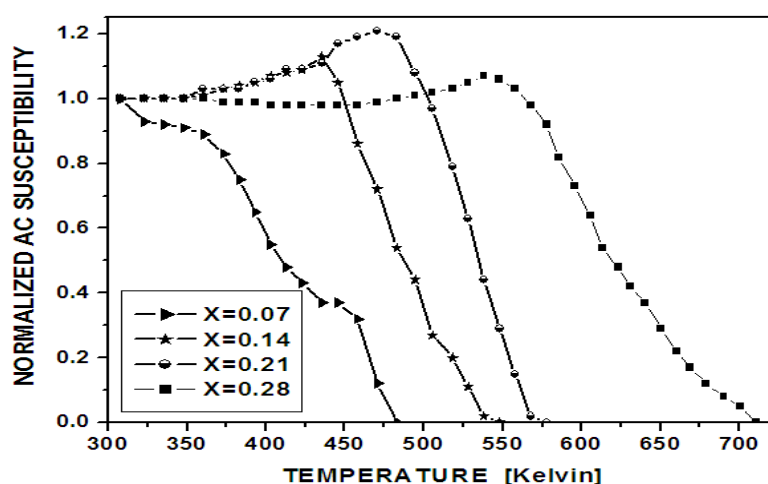


Fig. 4. Variation of normalized a.c.susceptibility with temperature of $\text{Li}_X\text{Mg}_{0.7-2X}\text{Zn}_{0.3}\text{Fe}_{2+X}\text{O}_4$ with $X=0.07, 0.14, 0.21$ and 0.28 .

CONCLUSION

The $\text{Li}_X\text{Mg}_{0.7-2X}\text{Zn}_{0.3}\text{Fe}_{2+X}\text{O}_4$ synthesized using sucrose precursor were found to have spinel nature with the average particle size ranging from 52 to 84 nm. The co-substitution of lithium and iron ions for Mg^{2+} contracted the lattice parameter and cation radii due to the difference in ionic sizes. An unexpected result was that the values of force constants increased by the extension in bond lengths due to the formation of stronger bonds by O^{2-} with metal ions. Squareness of the B-H loop and magnetization of the material diminished with the increase in Mg^{2+} concentration. The samples with $X=0$ and 0.07 may possess super paramagnetic particles, while all the other samples may have single domain particles. The T_c value decreased with increase in magnesium concentration due to the weaker A-B interaction.

Acknowledgements

One of the authors Dr. Vijaya Puri gratefully acknowledges the award of Research Scientist 'C' by University Grants Commission, India.

REFERENCES

- [1] El Badawy; El-Sharawy; CJ Koga, *IEEE Trans. Microw. Theo. Tech.*, **1991**, 39, 204.
- [2] E F Schloemann, *IEEE Trans. Mag.*, **2001**, 37, 2386.
- [3] AN Yusoff, MH Abdullah, *J. Magn. Magn. Mater.*, **2004**, 269, 271.
- [4] JS Baijal, S Phanjoubam, D Kothari, *Solid. State. Comm.*, **1992**, 83, 679.
- [5] LI Koshkin, NF Makienko, AD Kharlamov, *Sov. Phys. Solid State*, **1977**, 19, 551.
- [6] AM El-Sayed, *Mater. Chem. Phys.*, **2003**, 82, 583.
- [7] KK Jain, P Kishan, *IETE Technical review*, **1997**, 14, 373.
- [8] P Pramanik, *Bull. Mater. Sci.* **1999**, 22, 335.
- [9] RD Waldron, *Phys. Rev. B*, **1955**, 99, 1727.
- [10] SR Sawant, SS Suryavanshi, *Current Sci.*, **1988**, 57, 12.
- [11] MC Chhantbar, UN Trivedi, PV Tanna, HJ Shah, RP Vara, HH Joshi, KB Modi, *Indian J. Phys.* **2004**, 78A, 321.
- [12] SA Patil, VC Mahajan, AK Ghatage, SD Lotke, *Mater. Chem. Phys.*, **1998**, 57, 86.
- [13] CM Srivastava, TT Srinivasan, *J. Appl. Phys.* **1982**, 53, 8184.
- [14] SS Bellad, Ph.D. Thesis, **1999**, Shivaji University Kolhapur (India).
- [15] RV Mangalaraja, S Ananthakumar, P Manohar, FD Gnanam, *Mater. Lett.*, **2003**, 57, 2666.
- [16] BP Ladgaonkar, PN Vasambekar, AS Vaingankar, *J. Magn. Magn. Mater.* **2000**, 210, 289.
- [17] MC Sable, BK Labde, NR Shamkuwar, *Bull. Mater. Sci.*, **2005**, 28, 35.